# Second-order Raman spectra of SiC: Experimental and theoretical results from *ab initio* phonon calculations

W. Windl, K. Karch, P. Pavone, O. Schütt, and D. Strauch
*Institut für Theoretische Physik, Universität Regensburg, D-93040 Regensburg, Germany*

W. H. Weber, K. C. Hass, and L. Rimai
*Physics Department MD-3028/SRL, Ford Research Laboratory, Dearborn Michigan 48121-2053*
(Received 30 November 1993)

We report experimental and theoretical low-temperature second-order Raman spectra of 3C-SiC. Similar to the spectra of other group-IV and III-V semiconductors the $\Gamma_1$ spectrum is strong, and the $\Gamma_{12}$ and $\Gamma_{15}$ spectra are very weak. The theoretical Raman spectra have been calculated using *ab initio* phonon eigensolutions and phenomenological polarizability coefficients. Good agreement between theory and experiment has been obtained. The $\Gamma_1$ spectrum exhibits three distinct peaks at 1302, 1400, and 1619 $cm^{-1}$ which occur in the gaps of the overtone density of states. This exemplifies the importance of taking into account the coupling matrix elements rather than simply relying on the one-to-one correspondence between the overtone density of states and the $\Gamma_1$ Raman spectrum, which is commonly done for ZnS-type semiconductors.

## I. INTRODUCTION

Because of its salient mechanical, chemical, thermal, and electronic properties silicon carbide (SiC) is considered to be a promising material for electronic and optical devices for use in high-power, high-speed, high-temperature, high-frequency, and hard-radiation applications.[1,2] SiC is also an interesting material to study because of its special position among the wide-gap semiconductors: It is the only IV-IV compound which forms stable long-range ordered structures. However, despite the technological interest and the physical peculiarities SiC has not been subject to the same thorough theoretical and experimental studies as for example the crystals of its constituent elements carbon and silicon.

With regard to the crystal structure of SiC, a large number of polytypes with hexagonal or orthorhombic symmetry has been reported so far[3] besides the cubic phase on which we will concentrate in this work. Furthermore, considerable efforts have been undertaken to investigate the mechanism of the polytype growth and to determine the crystal structure of specimens. In particular, x-ray diffraction, high-resolution transmission electron microscopy and first-order Raman spectroscopy have been used to characterize the polytype structure. This work focuses on the second-order Raman scattering which gives also an insight into the lattice-dynamical properties and ultimately information on the strength and range of interatomic forces.[4]

The structure of the paper is the following: After this introduction we summarize the theory of the two-phonon Raman scattering in Sec. II. Experimental details and results are reported in Sec. III. Section IV contains the background of the *ab initio* lattice dynamics, on which the calculation of the Raman spectra is based, our phenomenological model for the second-order polarizability coefficients, and the resulting theoretical Raman spectra. The results are compared, discussed, and summarized in Sec. V.

## II. SHORT THEORY OF TWO-PHONON RAMAN SCATTERING

Raman scattering of light by lattice vibrations of a crystal depends on the modulation of the electronic susceptibility $\chi$ by phonons.[5,6] In fact, $\chi$ can be expressed as a power series in terms of phonon displacements $\mathbf{u}\binom{l}{\kappa}$ where $\binom{l}{\kappa}$ indicates the $\kappa$th sublattice in the $l$th unit cell,

$$\chi_{\alpha\beta} = P_{\alpha\beta} + \sum_{l\kappa\gamma} P_{\alpha\beta,\gamma}\binom{l}{\kappa}\, u_\gamma\binom{l}{\kappa} + \frac{1}{2}\sum_{l\kappa l'\kappa'\gamma\delta} P_{\alpha\beta,\gamma\delta}\binom{l\ l'}{\kappa\ \kappa'}\, u_\gamma\binom{l}{\kappa}\, u_\delta\binom{l'}{\kappa'} + \cdots . \tag{1}$$

The second-order Raman polarizability coefficients are defined as[5]

$$P_{\alpha\beta}(\mathbf{q}jj') = \frac{\hbar}{2\sqrt{\omega(\mathbf{q}j)\,\omega(\mathbf{q}j')}} \sum_{l\kappa\kappa'\gamma\delta} P_{\alpha\beta,\gamma\delta}\binom{0\ l}{\kappa\ \kappa'} \times w_\gamma(\kappa|\mathbf{q}j)\, w^*_\delta(\kappa'|\mathbf{q}j')\, e^{i\mathbf{q}\cdot[\mathbf{R}\binom{l}{\kappa'}-\mathbf{R}\binom{0}{\kappa}]}, \tag{2}$$

where $\mathbf{w}(\kappa|\mathbf{q}j)$ represents a normal-mode eigenvector and $\omega(\mathbf{q}j)$ the corresponding frequency; the vector $\mathbf{R}\binom{l}{\kappa}$ indicates an atomic site.

The scattering cross section depends upon the polarizations of the light and upon the crystal orientation. If the polarization vectors of the electric field of the incident and scattered light are denoted by $\mathbf{e}^i$ and $\mathbf{e}^f$, re-

 

spectively, the cross section can be written as[5]

$$\frac{d^2\sigma}{d\omega d\Omega} = \frac{\omega_i \omega_f^3}{c^4} \sum_{\alpha\beta\gamma\delta} e_\alpha^i e_\beta^f e_\gamma^i e_\delta^f I_{\alpha\beta\gamma\delta}(\omega), \quad (3)$$

where

$$I_{\alpha\beta\gamma\delta}(\omega) = \frac{1}{2} \sum_{\mathbf{q}jj'} P_{\alpha\beta}(\mathbf{q}jj') P^*_{\gamma\delta}(\mathbf{q}jj') \times \delta[\omega(\mathbf{q}j) + \omega(\mathbf{q}j') - \omega] \quad (4)$$

is the second-order Raman tensor at zero temperature.

## III. EXPERIMENT

The SiC samples were epitaxial films grown by chemical vapor deposition on Si(100) substrates.[7] Two different films were examined, one 3 $\mu$m thick from Cree Research Corporation and one 12 $\mu$m thick from the NASA Lewis Laboratory; the same results were obtained for each sample. Raman spectra were recorded using the 514.5-nm argon laser, a SPEX triple spectrometer, and an intensified array detector system as described in more detail elsewhere.[8] Data were taken with the samples at room temperature and usually in an atmosphere purged with Ar to remove the Raman lines of air. The spectra are corrected for the polarization dependence of the spectrometer throughput; thus relative intensities amongst different spectra at the same Raman shift can be directly compared. The laser power was 50 mW, focused to a spot size of $\sim$30 $\mu$m, and the spectral resolution was $\sim$7 cm$^{-1}$. No laser heating is expected since SiC is fairly transparent at 514.5 nm. In the region above $\sim$1100 cm$^{-1}$ spectra from the SiC films could be obtained without measurable interference from the Si substrate. At lower frequencies, however, the second-order Si spectrum far exceeds that from the SiC film. In order to obtain useful results, it was thus necessary to remove the films from the substrates. This was done by etching away the silicon in an 80 °C solution of KOH. The films still had residual surface roughness that was apparent both from the large Rayleigh scattered signal and from the lack of complete extinction of the forbidden TO phonon.[9]

The $xy$ ($\Gamma_{15}$) and $x'y'$ ($\Gamma_{12}$) spectra are too weak to be reliably measured in the frequency regime below 1000 cm$^{-1}$ and, in addition, are obscured by the first-order lines. The LO line is responsible for the steep rise in the $xy$ and $x'y'$ spectra near 1000 cm$^{-1}$, and no attempt has been made to remove it from these spectra.

Due to polarization leakage and surface roughness scattering the $xx$ ($\Gamma_1 + \Gamma_{12}$) spectrum exhibits strong LO and TO lines. These lines have been fitted to Lorentzians and subtracted from the spectra. The noisy structures near 790 and 970 cm$^{-1}$ are the residuals left over from this process. The peak at about 740 cm$^{-1}$, however, is a robust feature that is clearly present even before the TO line has been subtracted. In addition to the first-order lines, there is excess scattering in the region below $\sim$400 cm$^{-1}$. We suspect this scattering is related to the surface roughness, since it is much larger in the very rough SiC-on-Si films we have made by laser ablation.[10] This excess scattering is also completely absent from bare Si wafers with smooth surfaces.

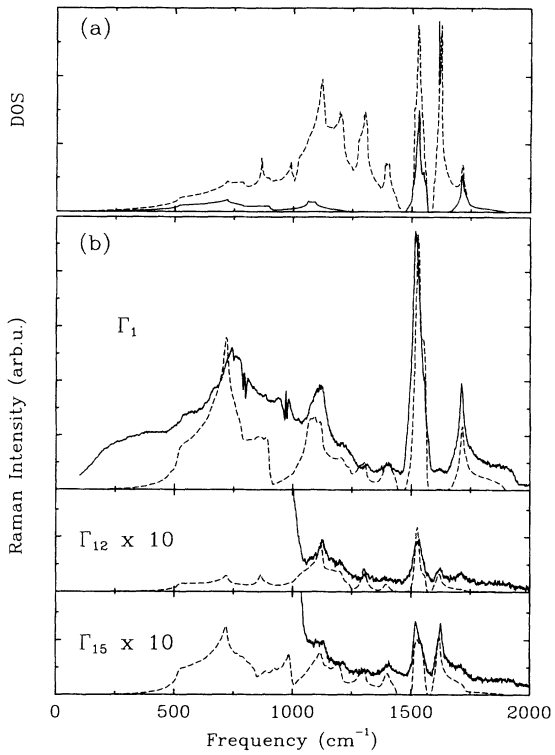


FIG. 1. (a) Two-phonon (dashed line) and overtone (solid line) density of states; (b) experimental reduced (solid lines) and theoretical zero-temperature (dashed lines) normalized polarized Raman spectra of SiC.

To simulate zero-temperature data we have divided the experimental spectra by $[1 + n(\omega)]^2$, where $n(\omega) = [\exp(\hbar\omega/2kT) - 1]^{-1}$ is the Bose-Einstein statistical factor for a phonon at $\omega/2$. This process is correct for overtone scattering, but only approximate for combinations of phonons from different branches.[11] Difference scattering is expected to be weak since only the lowest-energy acoustic phonons ($\hbar\omega < kT \approx 200$ cm$^{-1}$) can participate at room temperature. The reduced data are shown as the solid lines in Fig. 1(b), which are compared with the calculated results (dashed lines). Note that in the top panel the $xx$ spectrum is only approximately $\Gamma_1$, since it contains a small contribution (less than 10%) from $\Gamma_{12}$.

## IV. THEORETICAL CALCULATION

The eigenvectors and eigenvalues which are necessary to evaluate Eq. (2) have been calculated using the density-functional perturbation theory implemented within the plane-wave pseudopotential method.[12–14] For the exchange-correlation energy we used the local-density expression of Ref. 15. The norm-conserving pseudopotentials have been constructed following the scheme of Troullier and Martins.[16] A plane-wave basis with a kinetic energy cutoff of 36 Ry (corresponding to about 790

TABLE I. Parameter ratios giving the best agreement of the theoretical spectra with the experimental ones. We only report the parameters relative to each other because of the arbitrary units in all the experimental spectra.

| $\Pi_2^{(1)}/\Pi_1^{(1)}$ | $\Pi_2^{(12)}/\Pi_1^{(12)}$ | $P_{41}/P_{44}$ | $P_{42}/P_{44}$ | $P_{45}/P_{44}$ |
|---|---|---|---|---|
| 0.380 | 2.029 | −0.028 | −0.926 | −0.175 |

plane waves) has been chosen. With this plane-wave basis set the phonon dispersion converges to within a relative deviation of less than 1.5%. For the summation in reciprocal space we have used ten Chadi-Cohen points.[17]

Our *ab initio* calculations show that the lattice-dynamical properties of SiC are intermediate between those of diamond and Si, even though not the average of the two. The detailed description of the lattice dynamics of SiC will be reported elsewhere.[18]

For each shell of neighbors there are 81 polarizability coefficients $P_{\alpha\beta,\gamma\delta}\left(\begin{smallmatrix}0 & l\\ \kappa & \kappa'\end{smallmatrix}\right)$ which are partially related by symmetry properties. In a recent paper[19] it has been shown that restriction of the interactions up to just the nearest neighbors is sufficient in order to reproduce the Raman spectra of diamond-type semiconductors. Within this approximation using the invariance of the crystal lattice under the symmetry operations of the $T_d$ (zincblende) point group, one is left with only eight different coefficients. Using Voigt's notation[5] for the neighbor pair at $\mathbf{R}\left(\begin{smallmatrix}0\\ 1\end{smallmatrix}\right) = (0,0,0)$ and $\mathbf{R}\left(\begin{smallmatrix}0\\ 2\end{smallmatrix}\right) = (1,1,1)\,a/4$, we get

$$P_{IJ}\left(\begin{smallmatrix}0 & 0\\ 1 & 2\end{smallmatrix}\right) = \left(\begin{array}{ccc|ccc} P_{11} & P_{12} & P_{12} & P_{14} & P_{15} & P_{15} \\ P_{12} & P_{11} & P_{12} & P_{15} & P_{14} & P_{15} \\ P_{12} & P_{12} & P_{11} & P_{15} & P_{15} & P_{14} \\ \hline P_{41} & P_{42} & P_{42} & P_{44} & P_{45} & P_{45} \\ P_{42} & P_{41} & P_{42} & P_{45} & P_{44} & P_{45} \\ P_{42} & P_{42} & P_{41} & P_{45} & P_{45} & P_{44} \end{array}\right). \quad (5)$$

Of the three representations of the Raman spectrum in the $T_d$ point-group symmetry, the $\Gamma_1$ spectrum is expressed in terms of the parameters $\Pi_1^{(1)} = P_{11} + 2P_{12}$ and $\Pi_2^{(1)} = P_{14} + 2P_{15}$, the $\Gamma_{12}$ spectrum by the parameters $\Pi_1^{(12)} = P_{11} - P_{12}$ and $\Pi_2^{(12)} = P_{14} - P_{15}$, and the $\Gamma_{15}$ spectrum by the parameters $P_{41}$, $P_{42}$, $P_{44}$, and $P_{45}$.[20]

These parameters have been obtained by a least-squares adjustment of the theoretical spectra in the high-frequency regime ($> 1000$ cm$^{-1}$) with a constant experimental background taken out. The resulting parameters are given in Table I, and the corresponding second-order Raman spectra are shown together with the experimental curves in Fig. 1(b). In order to take into account resolution and phonon lifetime effects, we have performed a convolution of the calculated spectra with a Gaussian of linewidth $\Delta\omega = 7.6$ cm$^{-1}$.

## V. DISCUSSION AND SUMMARY

The agreement between experimental and theoretical scattering intensities is generally good. Referring to Figs. 1(a) and 1(b), the similarity between the overtone density of states and the $\Gamma_1$ spectrum which is dominated by overtones[21] can clearly be seen. However, there is a significant difference between the overtone density of states and the corresponding $\Gamma_1$ spectra that points out the necessity of including the coupling matrix elements in the calculation of the Raman spectra: While the overtone density of states has a gap between 1256 cm$^{-1}$ and 1474 cm$^{-1}$ there are two distinct peaks at 1302 cm$^{-1}$ and 1400 cm$^{-1}$ in the $\Gamma_1$ spectrum; the same holds for the peak at 1619 cm$^{-1}$ in the gap between 1567 cm$^{-1}$ and 1651 cm$^{-1}$ which is reproduced by our calculation with only a very weak intensity. These peaks must be due to combinations of phonons from *different* branches and *cannot* be caused by overtones.

Noticeable differences between theory and experiment occur in the frequency region below 1000 cm$^{-1}$. These could have many causes: The fit-and-subtract procedure to remove the first-order lines may have obscured the shoulder near 850 cm$^{-1}$. There may be excess scattering due to surface roughness or other defect-activated one-phonon scattering. Some difference processes may be contributing more than we anticipate. And, finally, the coupling matrix elements ranging beyond the nearest neighbors, which we have neglected, may need to be included.

Our present investigation supports the fact that a complete *ab initio* calculation of the lattice dynamics is necessary for a correct interpretation of experimental phonon spectra: To emphasize how sensitive the second-order Raman spectrum is to the underlying phonon model, we present in Fig. 2 a comparison of the experimental $xx$ spectrum with the overtone density of states for SiC computed from the shell-model force constants of Ref. 22. The dispersion curves along the main symmetry direc-

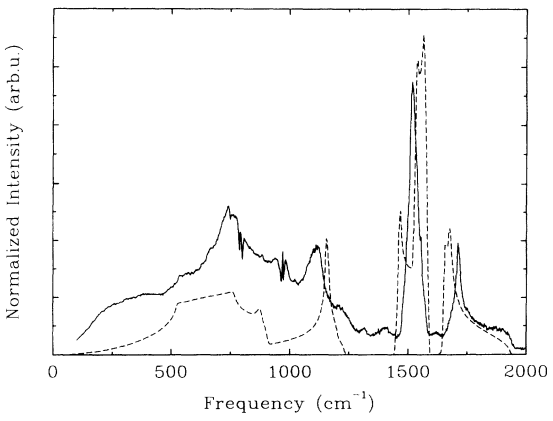


FIG. 2. Normalized $xx$ scattering from SiC (solid curve) compared with the overtone density of states calculated from the model of Ref. 22 (dashed curve).

tions in Ref. 22 are quite similar to those in the present work, and both models agree equally well with the limited dispersion data available. Nevertheless, the overtone density of states in Fig. 2 differs significantly from the full *ab initio* results in Fig. 1(a) and is much less successful for describing the second-order scattering. The largest discrepancy occurs in the vicinity of 1500 $cm^{-1}$ where the parametrized shell model incorrectly predicts that the TO phonons give rise to two principal peaks separated by 100 $cm^{-1}$. The shell model also predicts the wrong peak positions in the LO region and for the highest-frequency acoustic modes.

## ACKNOWLEDGMENTS

We wish to thank L. G. Matus of the NASA Lewis Research Laboratory for providing one of the samples used in this study. This work has been supported in part by the *Deutsche Forschungsgemeinschaft* under Contract No. SCHR123/8.

[1] R. F. Davis, Z. Sitar, B. E. Williams, H. S. Kong, H. J. Kim, J. W. Palmour, J. A. Edmond, J. Ryu, J. T. Glass, and C. H. Carter, Jr., Mater. Sci. Eng. B **1**, 77 (1988).

[2] W. J. Choyke, in *The Physics and Chemistry of Carbides, Nitrides and Borides,* edited by R. Freer, Vol. 185 of *Nato Advanced Study Institute, Series E: Appl. Sci.* (Kluwer, Dordrecht, 1990).

[3] N. W. Jepps and T. F. Page, *Crystal Growth and Characterisation of Polytype Structures*, in *Progress in Crystal Growth and Characterisation*, edited by P. Krishna (Pergamon, New York, 1983) Vol. 7, p. 259.

[4] K. Karch, Ph.D. thesis, Universität Regensburg, 1993.

[5] M. Born and K. Huang, *Dynamical Theory of Crystal Lattices* (Oxford University Press, Oxford, 1954).

[6] R. Loudon, Adv. Phys. **13**, 423 (1964).

[7] J. A. Powell and L. G. Matus, in *Amorphous and Crystalline Silicon Carbide and Related Materials*, Springer Proceedings in Physics Vol. 34, edited by G. L. Harris and C. Y.-W. Yang (Springer, Berlin, 1989), p. 2 and p. 40.

[8] J. R. McBride, K. C. Hass, and W. H. Weber, Phys. Rev. B **44**, 5016 (1991).

[9] Z. C. Feng, A. J. Mascarenhas, W. J. Choyke, and J. A. Powell, J. Appl. Phys. **64**, 3176 (1988).

[10] L. Rimai, R. Ager, E. M. Logothetis, W. H. Weber, and J. Hangas, in *Wide Band Gap Semiconductors*, edited by T. D. Moustakas, J. I. Pankove, and Y. Hamakawa, MRS Symposia Proceedings No. 242 (Materials Research Society, Pittsburgh, 1992), p. 549.

[11] M. Cardona, in *Light Scattering in Solids II,* Vol. 50 in *Topics in Applied Physics,* edited by M. Cardona and G. Güntherodt (Springer-Verlag, Berlin, 1982), p. 19 (in particular, pp. 31–36).

[12] S. Baroni, P. Giannozzi, and A. Testa, Phys. Rev. Lett. **58**, 1861 (1987).

[13] P. Giannozzi, S. de Gironcoli, P. Pavone, and S. Baroni, Phys. Rev. B **43**, 7231 (1991).

[14] P. Pavone, K. Karch, O. Schütt, D. Strauch, W. Windl, P. Giannozzi, and S. Baroni, Phys. Rev. B **48**, 3156 (1993).

[15] J. Perdew and A. Zunger, Phys. Rev. B **23**, 5048 (1981).

[16] N. Troullier and J. L. Martins, Phys. Rev. B **43**, 1993 (1991).

[17] D. J. Chadi and M. L. Cohen, Phys. Rev. B **8**, 5747 (1973).

[18] K. Karch, P. Pavone, W. Windl, O. Schütt, and D. Strauch (unpublished).

[19] W. Windl, P. Pavone, K. Karch, O. Schütt, D. Strauch, P. Giannozzi, and S. Baroni, Phys. Rev. B **48**, 3164 (1993).

[20] H. Bilz, D. Strauch, and R. K. Wehner, *Vibrational Infrared and Raman Spectra of Non-Metals, Handbuch der Physik, Vol. 25/2d: Licht und Materie*, edited by S. Flügge (Springer, Berlin, 1984), in particular, p. 148.

[21] J. L. Birman, Phys. Rev. **127**, 1093 (1962); **131**, 1489 (1963).

[22] C. Cheng, K. Kunc, and V. Heine, Phys. Rev. B **39**, 5892 (1989).